



Sharif University of Technology

Scientia Iranica

Transactions A: Civil Engineering

www.sciencedirect.com



Robust multi-objective optimization design of TMD control device to reduce tall building responses against earthquake excitations using genetic algorithms

S. Pourzeynali^{a,*}, S. Salimi^{b,1}, H. Eimani Kalesar^{b,2}

^a Department of Civil Engineering, Faculty of Engineering, University of Guilan, Rasht, Islamic Republic of Iran

^b Department of Civil Engineering, Faculty of Engineering, University of Mohaghegh-Ardebili, Ardebil, Islamic Republic of Iran

Received 8 October 2011; revised 4 August 2012; accepted 26 November 2012

KEYWORDS

Tuned mass damper;
Multi-objective optimization;
Genetic algorithms;
Robust design optimization;
Earthquake excitation.

Abstract Tuned Mass Dampers (TMDs) are a well-accepted control device widely used by the civil engineering community. The main purpose of this study is the robust multi-objective optimization design of this device using Genetic Algorithms (GAs) to control the structural vibrations against earthquakes. To enhance the performance of the TMD system, its parameters, including mass, stiffness, and damping ratio, have been optimally designed using multi-objective genetic algorithms. For doing this, three non-commensurable objective functions, namely: maximum displacement, maximum velocity, and maximum acceleration of each floor, are considered, which are to be minimized simultaneously. For this purpose, a fast and elitist Non-dominated Sorting Genetic Algorithm (NSGA-II) approach is used to find a set of Pareto-optimal solutions. Moreover, in order to take into account the uncertainties existing in the system, a robust design optimization procedure is performed using the Hammersley sequence sampling approach. In this study, the example building is modeled as a 3-D frame, and its responses are evaluated using coupled multi-mode analysis. From the numerical results of the study, it is found that the robust TMD system is capable of providing a reduction of about 28% on maximum displacement of the building.

© 2013 Sharif University of Technology. Production and hosting by Elsevier B.V. All rights reserved.

1. Introduction

During past decades, reduction of the undesired vibrations of structures due to environmental dynamic hazards such as earthquakes was a meaningful and challenging task for structural engineers. Various strategies and theories have been developed to approach this goal over the years. Use of control

systems is one of these strategies to enhance structural performance against vibration excitations [1–4]. The main purpose of control systems is to reduce structural responses, such as displacement, velocity and acceleration. Control systems are divided into four groups of passive, semi active, active, and hybrid systems, based on the rate of energy consumption and their kind of installation in the main structure [5]. The passive systems dissipate vibration excitations without using any energy source. Therefore, as these systems add no energy to the structure, they are not able to make the structure unstable. Another advantage of these systems is the low cost of repair and maintenance. In this study, the robust multi-objective optimization design of a Tuned Mass Damper (TMD) control device is investigated as a passive control system. The TMD system is a well-accepted device for controlling flexible structures, particularly, tall buildings [6]. Although the TMD control system may be considered a hybrid of a tuned dynamic absorber, including a mass block and a spring combined with a viscous damper, in the engineering community, it is known as a passive control system [7,8]. The theory of TMD was used for the first time by Frahm in 1909 [9]. A typical kind of TMD system consists of a mass block,

* Corresponding author. Tel.: +98 131 6690270; fax: +98 131 6690271, Mobile: +98 9113310919.

E-mail addresses: pourzeynali@guilan.ac.ir (S. Pourzeynali), shide.salimi@gmail.com (S. Salimi), hek@uma.ac.ir (H. Eimani Kalesar).

¹ Present address: # 1403, 1190 Rue Du Fort, Montreal, Quebec, H3H 2B5, Canada. Tel.: +1 514 649 5020, Mobile: +98 9125825020.

² Mobile: +98 9143512509.

Peer review under responsibility of Sharif University of Technology.



Production and hosting by Elsevier

a fluid viscous damper and a spring connected to the main structure on one of its degrees of freedom. The natural frequency of the TMD is tuned to the resonant frequency of the main structure, so, a large amount of entrance energy is transferred to the TMD [10,11]. The performance of the TMD is based on the optimal robust design of its parameters, namely, mass, stiffness, and damping ratio, and the location of this system on the main structure. The TMDs are undoubtedly reliable and simple, and they do not require an external power source, so, the cost of their construction is low [12]. The design of the TMD system, which is related to the special condition of the vibration and frequency of a structure, can cause incompatibility with possible changes in specifications of the structure or loading conditions. These problems led to the use of active and semi-active systems, which are more compatible with changes in conditions.

Different classical and robust control algorithms have been proposed to reduce high rise buildings responses [13–15], the most common being LQR, LQG, clipped control, sliding mode control, pole assignment, H_2 , H_∞ control, fuzzy logic control, and so on [5,16–19]. Most control design methods are based on optimization techniques of maximizing the performance of systems through minimizing structural response quantities [11,20–23].

In the present study, the parameters of the TMD will be optimally designed using multi-objective genetic algorithms for a 12-story realistic building through both deterministic and robust design procedures. There are trade-offs between some objective functions through optimal design of this device, therefore, it is not possible to choose an appropriate optimum design reflecting the compromise of the designer's choice concerning the absolute values of the objective functions. Consequently, this problem can be formulated as a Multi-objective Optimization Problem (MOP). Three non-commensurable objective functions, namely, maximum displacement, maximum velocity, and maximum acceleration of each floor, are considered, which are to be minimized simultaneously.

Moreover, in the optimal design procedure of a system, it is required that the uncertainties which may exist in the system are to be taken into account. This consideration can be performed through a Robust Design Optimization (RDO) procedure. This method is based on a non-deterministic optimization approach, through which probabilistic uncertainties can be considered for uncertain parameters, and the stochastic optimal design process can be performed for the system. The Hammersley Sequence Sampling (HSS) method, which is a direct and simple numerical method, is used in the present study to perform the RDO procedure. Finally, the robust optimal values of the TMD parameters are evaluated for the sample building structure.

2. Mathematical modeling of the building

For an n -story building structure with a TMD system installed on its top floor, subjected to earthquake horizontal acceleration components, as shown in Figure 1, the equations of motion can be given as [6]:

$$[M]\{\ddot{u}(t)\} + [C]\{\dot{u}(t)\} + [K]\{u(t)\} = -[M][R]\{\ddot{u}_g(t)\} + \{l\}(c_d\dot{u}_{rd} + k_d u_{rd}), \quad (1)$$

$$m_d\ddot{u}_{rd}(t) + c_d\dot{u}_{rd}(t) + k_d u_{rd}(t) = -m_d\{l\}^T\{\ddot{u}(t)\} - m_d\{\ddot{u}_{gx}(t)\}, \quad (2)$$

where $[M]$, $[C]$, and $[K]$ are the $3n \times 3n$ mass, damping, and stiffness matrices of the main structure, respectively; n is the

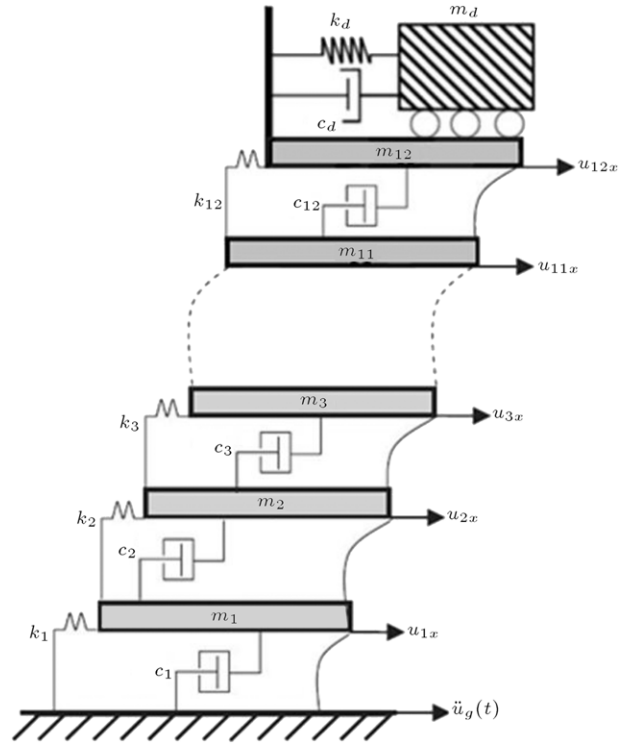


Figure 1: Example of realistic building model and the TMD mounted on its top floor.

number of stories; and $\{u(t)\}$ is the $3n \times 1$ displacement vector of the building, with respect to the ground, expressed as:

$$\{u(t)\} = \begin{Bmatrix} \{u_x(t)\} \\ \{u_y(t)\} \\ \{u_\theta(t)\} \end{Bmatrix}, \quad (3)$$

where $\{u_x(t)\}$, $\{u_y(t)\}$ and $\{u_\theta(t)\}$ are the $n \times 1$ displacement vectors of the building in x , y , and θ directions, respectively; $u_{rd}(t)$ is the relative displacement of the TMD, with respect to the top floor; m_d , k_d , and c_d are the mass, stiffness, and damping of the TMD; and $[R]$ is the $3n \times 3$ influence matrix, given in the following:

$$[R] = \begin{bmatrix} \{1\} & \{0\} & \{0\} \\ \{0\} & \{1\} & \{0\} \\ \{0\} & \{0\} & \{1\} \end{bmatrix}, \quad \{1\}_{n \times 1} = \{1, 1, \dots, 1\}^T, \quad (4)$$

$$\{0\}_{n \times 1} = \{0, 0, \dots, 0\}^T.$$

$\{l\}$ is the $3n \times 1$ location vector of the control device; and $\{\ddot{u}_g(t)\}$ shows the acceleration of the earthquake acting on the base of the main structure, which can be expressed as:

$$\{\ddot{u}_g(t)\} = \begin{Bmatrix} \ddot{u}_{gx}(t) \\ \ddot{u}_{gy}(t) \\ \ddot{u}_{g\theta}(t) \end{Bmatrix}, \quad (5)$$

where $\ddot{u}_{gx}(t)$ and $\ddot{u}_{gy}(t)$ are the horizontal components of the earthquake accelerations in x and y directions, and $\ddot{u}_{g\theta}(t)$ is that of the torsional component. It is noted that in this study, the control device is considered only in a x direction.

The simplest procedure to define the mass properties of the building is to assume that the entire mass of each floor is concentrated at the mass center of the floor (rigid floor

assumption). Therefore, the mass matrix of the building will be a lumped matrix, given in the following [24]:

$$[M] = \begin{bmatrix} m_1 & \cdots & 0 & 0 \\ \vdots & m_2 & & 0 \\ 0 & & \ddots & \vdots \\ 0 & 0 & \cdots & m_{3n} \end{bmatrix}, \quad (6)$$

where m_i is the i th story mass or mass moment of inertia. The damping matrix of the building is also considered to be a linear combination of mass and stiffness matrices, called Rayleigh damping, given as below [25]:

$$[C] = a_0[M] + b_0[K], \quad (7)$$

$$a_0 = 2\xi_i \frac{\omega_i \omega_j}{\omega_i + \omega_j}, \quad b_0 = 2\xi_j \frac{1}{\omega_i + \omega_j}, \quad (8)$$

in which a_0 and b_0 are the proportional coefficients; ω_i and ω_j are the structural modal frequencies of modes i and j , respectively; and ξ_i and ξ_j are the structural damping ratios for modes i and j , generally assumed to be the same, which means: $\xi_i = \xi_j = \xi$. It should be noted that these two modes should be selected such that all modes can contribute significantly to the final responses of the building. Therefore, it is recommended [26] that mode i is to be taken as the fundamental mode of the building, and mode j is to be set to the middle mode of the building.

The response of the building depends on its mode shapes and natural frequencies and can be estimated by considering the dominant modes of the building. Therefore, in this study, to obtain the building's uncontrolled responses, a classical modal analysis is performed. According to [27], the first vibrational mode is dominant in earthquake excitation if modal frequencies are well-separated. In this study, the first three frequencies of the sample building are very close. Thus, in order to reduce the analysis time of the optimization procedure using a genetic algorithm, the first three modes of the main structure in each direction are considered in the modal analysis of the building. Consequently, the displacement vector of the building can be expressed as:

$$\{u(t)\} = [\Phi]\{q(t)\}, \quad (9)$$

$$[\Phi] = [\{\phi\}_1 \quad \{\phi\}_2 \quad \{\phi\}_3], \quad \{q(t)\} = \begin{Bmatrix} q_1(t) \\ q_2(t) \\ q_3(t) \end{Bmatrix}, \quad (10)$$

where $\{\phi\}_i$ is the i th mode shape of the building, and $q_i(t)$ is the i th generalized modal coordinate of the structure. Therefore, the equation of motion of the building, considering the contribution of its first three modes, can be written as follows:

$$[\hat{M}]\{\ddot{q}(t)\} + [\hat{C}]\{\dot{q}(t)\} + [\hat{K}]\{q(t)\} = -[L]\{\ddot{u}_g(t)\} + [\Phi]^T\{l\}(c_d \dot{u}_{rd} + k_d u_{rd}), \quad (11)$$

in which,

$$[\hat{M}] = [\Phi]^T [M] [\Phi], \quad [\hat{C}] = [\Phi]^T [C] [\Phi], \\ [\hat{K}] = [\Phi]^T [K] [\Phi], \quad [L] = [\Phi]^T [M] [R]. \quad (12)$$

Now, by selecting the generalized modal coordinates, $\{q(t)\}$, $u_{rd}(t)$, and their time derivatives as the state variables, the state equation of the system (both Eqs. (2) and (11)) can be expressed in the standard state-space form, as follows [28]:

$$\{\dot{Z}(t)\} = [A]\{Z(t)\} + [D]\{\ddot{u}_g(t)\}, \quad (13)$$

in which $[A]$ is the system matrix; $[D]$ is the disturbance matrix; and $\{Z(t)\}$ is the state vector, given in the following:

$$[A] = \begin{bmatrix} [0]_{P \times P} & [I]_{P \times P} \\ -[\hat{M}]^{-1}[\hat{K}] & -[\hat{M}]^{-1}[\hat{C}] \end{bmatrix}_{2P \times 2P}, \quad (14)$$

where:

$$[\hat{M}] = \begin{bmatrix} \hat{M}_{1,1} & 0 & 0 & 0 \\ 0 & \hat{M}_{2,2} & 0 & 0 \\ 0 & 0 & \hat{M}_{3,3} & 0 \\ m_d \phi_{12,1} & m_d \phi_{12,2} & m_d \phi_{12,3} & m_d \end{bmatrix}, \\ [\hat{C}] = \begin{bmatrix} \hat{C}_{1,1} & \hat{C}_{1,2} & \hat{C}_{1,3} & -(\phi_{12,1}) c_d \\ \hat{C}_{2,1} & \hat{C}_{2,2} & \hat{C}_{2,3} & -(\phi_{12,2}) c_d \\ \hat{C}_{3,1} & \hat{C}_{3,2} & \hat{C}_{3,3} & -(\phi_{12,3}) c_d \\ 0 & 0 & 0 & c_d \end{bmatrix}, \\ [\hat{K}] = \begin{bmatrix} \hat{K}_{1,1} & \hat{K}_{1,2} & \hat{K}_{1,3} & -(\phi_{12,1}) k_d \\ \hat{K}_{2,1} & \hat{K}_{2,2} & \hat{K}_{2,3} & -(\phi_{12,2}) k_d \\ \hat{K}_{3,1} & \hat{K}_{3,2} & \hat{K}_{3,3} & -(\phi_{12,3}) k_d \\ 0 & 0 & 0 & k_d \end{bmatrix}, \\ [D] = \begin{bmatrix} [0]_{P \times (P-1)} \\ [\hat{D}] \end{bmatrix}, \\ [\hat{D}] = -[\hat{M}]^{-1} \begin{bmatrix} L_{1,1} & L_{1,2} & L_{1,3} \\ L_{2,1} & L_{2,2} & L_{2,3} \\ L_{3,1} & L_{3,2} & L_{3,3} \\ m_d & 0 & 0 \end{bmatrix}, \quad (16)$$

$$\{Z(t)\} = [q_1 \quad q_2 \quad q_3 \quad u_{rd} \quad \dot{q}_1 \quad \dot{q}_2 \quad \dot{q}_3 \quad \dot{u}_{rd}]^T, \quad (17)$$

where P is the half number of state variables, which is four in this study. In order to optimally design the parameters of TMD, its mass, m_d , is assumed as part of the total mass of the building (m_{Building}^t), expressed as:

$$m_d = m_0 \times m_{\text{Building}}^t, \quad (18)$$

in which m_0 is called the mass ratio of the TMD system. As mentioned earlier, in this research study, the TMD control device is considered to be installed on the top story of the building, and moves only in an x direction. Therefore, application of TMD can absorb the entrance energy only in this direction. For designing the TMD system, its frequency should be tuned close to the fundamental frequency of the building in an x direction, where the control device is installed. Therefore, the frequency of the TMD, ω_d , is expressed as:

$$\omega_d = (\beta \times \omega_{1x}), \quad (19)$$

where β is the frequency ratio of the TMD, and ω_{1x} is the fundamental frequency of the building in an x direction. Then, the damping coefficient of the TMD, c_d , can be expressed as:

$$c_d = 2 \times \xi_d \times \sqrt{(m_d \times k_d)}. \quad (20)$$

Therefore, parameters m_0 , β and ξ_d are considered as the design variables in the multi-objective optimization procedure using genetic algorithms.

3. Genetic algorithms and multi-objective optimization

Most engineering optimization problems are often very complex and difficult to solve using traditional optimization methods, and do not consider many simplifications. Traditional

optimization methods that are gradient based have many disadvantages. In recent years, use of evolutionary algorithms has been considered by many researchers in different optimization fields. The genetic algorithm was first proposed by Holland in 1975 [29]. Genetic Algorithms (GAs) are effective search methods in a very wide space that eventually lead to orientation towards finding an optimal solution. They can be used for solving a variety of optimization problems that are not well suited for standard optimization algorithms, including problems in which the objective function is discontinuous, non-differentiable, stochastic or highly nonlinear [30]. There are many differences between genetic algorithms and the traditional optimization methods; namely: GAs work with a population or set of points in a certain moment, while traditional optimization methods use a special point. This means that the GAs are processed a large number of schemes at one time. Unlike conventional optimization methods that use derivatives of functions, genetic algorithms just use objective function values. In these algorithms, the design space should be converted to the genetic space. Therefore, genetic algorithms work with a series of coded variables. The advantage of working with coded variables is that the codes have a basic capability to convert continuous space to discrete space. Another interesting point is that the principles of GAs are based on random processing, so the random operators investigate the search space comparatively. The main operational steps of genetic algorithms are: initialization, selection of chromosomes for reproduction, crossover between the chromosomes and producing the next generation, mutation for searching the other parts of the problem (to prevent early convergence), and insertion of children in the new population.

In recent years, the application of genetic algorithms has increased by specifying more and more capability, flexibility and speed. The main purpose in single-objective optimization problems is to find the values of design variables, in order to find the optimum value of a single objective function. In multi-objective optimization (which is also called vector optimization), the problem is to optimize more than one objective function, which are usually in conflict with each other in engineering optimization problems, so that the improvement of one leads to a worsening of the others. Therefore, multi-objective optimization offers an optimal set of solutions, rather than one optimal value. In this set of optimal solutions, no answer can be found which dominates the others. The optimal solutions are called Pareto points or the Pareto Front. In this set of optimal solutions, which one should be chosen is the most important question. This is not easy to answer. It involves much high-level information, which is often non-technical and experience-driven. However, if a set of many trade-off (conflicting scenarios) solutions is already available, then one can evaluate the pros and cons of each of these solutions based on all such non-technical and qualitative, yet still important, considerations, and compare them to make a choice. Thus, in a multi-objective optimization, ideally, an effort must be made to find the set of trade-off optimal solutions by considering all objectives to be important [31]. A routine method for solving multi-objective optimization problems is conversion of the multiple objective functions into one objective function. For this purpose, different methods are presented in scientific reports, from which the most widely used methods are: The weighted sum approach, ε -perturbation, Min–Max and the non-sorting genetic algorithm [24]. Genetic algorithms act well to solve multi-objective optimization problems, and recently, Srinivas and Deb [32] found a new algorithm based

on genetic algorithms for solving them. This method, called the non-dominated sorting genetic algorithm, or NSGA, is more powerful than previous algorithms in multi-objective optimization. Over the years, the main criticisms of the NSGA approach have been as follows [33]:

1. High computational complexity of non-dominated sorting: This method has a computational complexity of $O(mn^3)$, where M is the number of objectives and N is the population size. This makes NSGA computationally expensive for large population sizes.
2. Lack of elitism: The research results [34,35] show that elitism can significantly speed up the performance of the GA, which also can help in preventing the loss of good solutions once they are found.
3. Need for specifying the sharing parameter σ_{share} : Traditional mechanisms of ensuring diversity in a population so as to get a wide variety of equivalent solutions have relied mostly on the concept of sharing. The main problem with sharing is that it requires the specification of a sharing parameter (σ_{share}).

Because of the above difficulties of this method in solving optimization problems, the modified algorithm, called NSGA-II, was introduced by Deb a few years later, which acts better and faster to find non-dominated sorting solutions [33]. In multi-objective optimization, it was endeavored to find a design vector, $\{X^*\} = \{X_1^*, X_2^*, \dots, X_n^*\}^T$, which could optimize k objective functions, J_i , under m inequality and p equality constraints. Consequently, the multi-objective optimization can be briefly expressed as:

$$\begin{aligned} &\text{find } \{X^*\}, \text{ optimize } \{J(X)\}, \\ &\text{subject to } \begin{cases} g_i(X) \leq 0 & (i = 1, 2, \dots, m) \\ h_j(X) = 0 & (j = 1, 2, \dots, p) \end{cases} \end{aligned} \quad (21)$$

where $\{X^*\} \in \mathfrak{R}^n$ is the design variable vector; $\{J(X)\} = \{J_1(X), J_2(X), \dots, J_k(X)\}^T$ is the vector of the objective functions, so that $\{J(X)\} \in \mathfrak{R}^k$; and $g_i(X)$ and $h_j(X)$ are inequality and equality constraints, respectively.

In the present study, the multi-objective optimization is solved utilizing a computer program developed in MATLAB software. For a multi-objective GA optimizer, the following parameters, based on the authors' experiences, are chosen:

Probability of crossover, $P_c = 0.25$, and Probability of mutation, $P_m = 0.01$.

In optimization studies, including multi-objective optimization problems, the main objective is to find the global Pareto optimal solutions representing the best possible objective values. However, in practice, users may not always be interested in finding the global best solutions, particularly if these solutions are very sensitive to variable perturbations. In such cases, practitioners are interested in finding robust solutions that are less sensitive to small changes in variables [36].

4. Robust design of the TMD system

In many engineering problems, the mathematical models of systems considered in analyses and those of actual ones are different, due to uncertainties in the system. The performance of the systems could be sensitive to these uncertainties. Evidently, the uncertainties can affect the design performance, even though the design has been accomplished optimally. Therefore, in the optimal design procedure of a system, it is required that the uncertainties, which may exist in the

system, are to be taken into account. This consideration can be performed through the Robust Design Optimization (RDO) procedure. This method is based on a non-deterministic optimization approach, through which the probabilistic changes can be considered for uncertain parameters, and the stochastic optimal design process can be performed for the system. Therefore, some probabilistic metrics, which are often called random variables, are involved in the robust design [37]. In the RDO approach, the optimally evaluated random variables related to the stochastic performance of the system are expected to be less sensitive to the random variation of uncertain parameters.

In order to simulate the stochastic behaviour of the uncertain systems, there has been a great amount of research activity in the field, and the most prominent method used in many robust design methods is Monte Carlo simulation [38–40]. Monte Carlo Simulation (MCS) is a direct and simple numerical method, but can be computationally expensive. In this method, random samples are generated assuming some pre-defined probabilistic distributions for uncertain parameters. The system is then simulated with each of these randomly generated samples, and the percentage of cases produced in the failure region, defined by a limit state function, approximately reflects the probability of failure [39].

Let X be a random variable, then the prevailing model for uncertainties in stochastic randomness is the Probability Density Function (PDF), $f_X(x)$ or, equivalently, the cumulative distribution function (CDF), $F_X(x)$, where the subscript X refers to the random variable. This can be shown by [39]:

$$F_X(x) = \text{Pro}(X \leq x) = \int_{-\infty}^x f_X(x) dx, \quad (22)$$

where $\text{Pro}(\cdot)$ is the probability that an event ($X \leq x$) will occur. Some statistical moments, such as the first and the second moments, generally known as the mean value (also referred to as expected value) denoted by $E(X)$, and the variance denoted by $\sigma^2(X)$, respectively, are the most important ones. They can also be computed by [41]:

$$E(X) = \int_{-\infty}^{\infty} x dF_X(x) = \int_{-\infty}^{\infty} x f_X(x) dx, \quad (23)$$

and:

$$\sigma^2(X) = \int_{-\infty}^{\infty} (x - E(X))^2 f_X(x) dx. \quad (24)$$

In the case of discrete sampling, these equations can be readily represented as [41]:

$$E(X) \cong \frac{1}{N} \sum_{i=1}^N x_i, \quad (25)$$

and:

$$\sigma^2(X) \cong \frac{1}{N-1} \sum_{i=1}^N (x_i - E(X))^2, \quad (26)$$

where x_i is the i th sample and N is the total number of samples. In the Robust Design Optimization (RDO), the mean value and variance of each random variable should be minimized [42].

In order to improve the precision of this method, N should approach infinity, but it leads to computationally expensive problems. Therefore, there have been many research activities on sampling methods to reduce the number of samples keeping a high level of accuracy. Alternatively, the quasi-MCS has now been used in much research, which is known as Hammersley

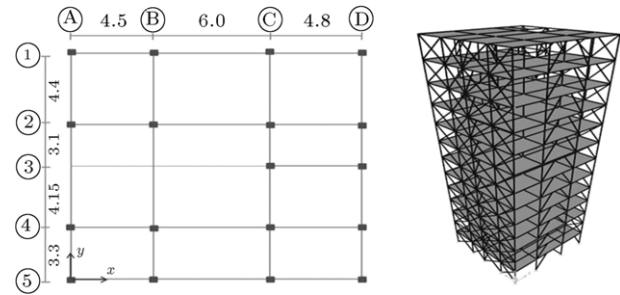


Figure 2: Typical plan and 3-D frame of the building.

Sequence Sampling (HSS) [39,40]. In the present study, HSS has been used to generate samples for the probability estimation of failures.

The goal of RDO is to minimize the mean and variance of each random variable. Therefore, the mean and its variability for each random variable should be minimized simultaneously [42]. In this paper, in order to minimize the mean and variance simultaneously, the objective function for each random variable is considered as:

$$J = \frac{E(X)}{E_0} + \frac{\sigma^2(X)}{\sigma_0^2}, \quad (27)$$

in which the mean and variance of the random variable are normalized by the desired mean (E_0) and the desired variance (σ_0^2), which can be chosen by the designer.

5. Numerical study

In order to investigate the performance of the proposed control devices in reducing the responses of building structures under earthquake excitations, a 12-story steel building, having plan dimensions of 15 m \times 15.5 m and height of 46.3 m, with residential application, located in the city of Rasht, Iran, is selected. Lateral resisting systems of the building against earthquake excitations are a combination of Intermediate Moment Frames (IMFs) and Eccentrically Braced Frames (EBFs) in an x -direction; and Special Concentrically Braced Frames (SCBFs) in a y -direction. This building is modeled as a 3-D frame to show more realistic behavior of the building and to control systems in earthquake events. A typical plan and building 3-D frame are shown in Figure 2.

For evaluating the performance of the proposed TMD control device and comparing the results, the above building is analyzed under the application of worldwide earthquake accelerograms. For time history dynamic analysis of the structure, necessary corrections are performed on the uncorrected accelerograms, including a band-pass filtering of low- and high-frequency noises, as well as the instrumental and base-line corrections. All corrected accelerograms are scaled individually, so that they are representative of accelerograms compatible with a design response spectrum [43]. In the present study, 16 worldwide strong ground motion accelerograms (presented in Table 1), with an effective duration of more than 10 s, have been selected, according to IBC2006 [43], and used in time history analyses.

Now, using the state-space equation of the building without any control system (Eq. (13)), the uncontrolled responses of the building are calculated under the application of the earthquake accelerograms given in Table 1. The maximum uncontrolled responses of the building, including the maximum

Table 1: Earthquake accelerograms considered in this study.

No.	Earthquake	Date	Effective duration (s)		Magnitude (Ms)	Corrected PGA (g)	Total duration (s)	Nearest fault distance (km)
			T	L				
1	Kocaeli	1999	36.615	37.2039	7.8	0.349	150.405	78.9
2	Chi-Chi	1999	35.876	39.9512	7.62	1.157	121	71.64
3	Landers	1992	35.4932	38.5746	7.4	0.284	120	80.5
4	Duze	1999	23.2598	26.2521	7.3	0.822	60	49.9
5	Cape Mendocino	1992	20.7865	19.847	7.1	1.497	44	44.6
6	Kobe	1995	13.1572	12.8662	6.9	0.694	40.96	26.4
7	Imperial valley	1979	19.4219	17.11	6.9	0.775	40	54.1
8	Garmkhan	1996	14.1873	16.095	6.8	0.08	26.88	–
9	Bam	2003	18.43	18.315	6.7	0.78	58.88	–
10	Northridge	1994	18.4292	19.71	6.7	0.877	34.99	71.1
11	San Fernando	1971	17.765	16.035	6.6	0.136	29.74	81.6
12	Coalinga	1983	21.3806	20.1946	6.5	0.733	40	55.2
13	Karebas	1997	12.9807	14.1065	6.3	0.28	23.04	–
14	Morgan hill	1984	21.2828	19.015	6.1	0.405	36	54.1
15	Zanjiran	1994	19.0637	15.685	6.1	1.07	26.88	–
16	Whittier narrows	1987	12.72	12.56	5.7	0.333	32.06	69.7

Table 2: Stories maximum uncontrolled responses (Dis = displacement (cm), Vel = velocity (m/s) and Acc = acceleration (m/s^2)).

Earthquakes		Stories of the building											
		1st	2nd	3rd	4th	5th	6th	7th	8th	9th	10th	11th	12th
Kobe	Dis	0.34	1.52	2.27	3.05	3.87	4.74	5.65	6.62	7.62	8.62	9.60	10.63
	Vel	0.02	0.07	0.10	0.14	0.18	0.21	0.26	0.30	0.35	0.39	0.44	0.48
	Acc	0.08	0.36	0.53	0.72	0.91	1.12	1.33	1.57	1.81	2.05	2.29	2.54
Kocaeli	Dis	0.76	3.40	5.06	6.81	8.64	10.57	12.6	14.78	17.01	19.27	21.47	23.80
	Vel	0.04	0.16	0.24	0.32	0.41	0.50	0.59	0.69	0.80	0.90	1.00	1.11
	Acc	0.17	0.78	1.16	1.56	1.98	2.42	2.88	3.37	3.86	4.35	4.83	5.33
Chi-Chi	Dis	0.34	1.52	2.26	3.05	3.87	4.74	5.64	6.60	7.58	8.56	9.52	10.53
	Vel	0.01	0.06	0.10	0.13	0.16	0.20	0.24	0.28	0.32	0.37	0.41	0.46
	Acc	0.08	0.34	0.50	0.68	0.86	1.06	1.26	1.48	1.70	1.92	2.14	2.38
Morgan hill	Dis	0.20	0.90	1.33	1.79	2.28	2.78	3.32	3.89	4.47	5.05	5.63	6.23
	Vel	0.01	0.04	0.06	0.09	0.11	0.13	0.16	0.19	0.22	0.24	0.27	0.30
	Acc	0.09	0.40	0.59	0.80	1.01	1.24	1.48	1.73	1.99	2.26	2.51	2.78
San Fernando	Dis	0.12	0.53	0.79	1.07	1.35	1.66	1.97	2.31	2.66	3.01	3.36	3.72
	Vel	0.00	0.02	0.03	0.04	0.06	0.07	0.08	0.10	0.11	0.12	0.14	0.15
	Acc	0.04	0.20	0.29	0.39	0.50	0.61	0.72	0.85	0.97	1.10	1.22	1.35
Northridge	Dis	0.32	1.43	2.13	2.87	3.65	4.46	5.31	6.22	7.14	8.06	8.96	9.91
	Vel	0.01	0.06	0.08	0.11	0.14	0.18	0.21	0.25	0.28	0.32	0.36	0.40
	Acc	0.08	0.35	0.53	0.71	0.90	1.10	1.31	1.54	1.77	2.01	2.23	2.47
Coalinga	Dis	0.54	2.43	3.61	4.86	6.16	7.54	8.98	10.52	12.09	13.66	15.21	16.82
	Vel	0.02	0.10	0.15	0.20	0.25	0.31	0.37	0.43	0.50	0.56	0.63	0.69
	Acc	0.12	0.54	0.80	1.08	1.36	1.66	1.98	2.32	2.66	3.00	3.34	3.69
Average responses	Dis	0.34	1.52	2.27	3.05	3.87	4.74	5.65	6.62	7.61	8.61	9.58	10.61
	Vel	0.01	0.07	0.10	0.13	0.17	0.21	0.25	0.29	0.33	0.37	0.42	0.46
	Acc	0.09	0.41	0.60	0.81	1.03	1.26	1.51	1.76	2.03	2.29	2.55	2.82

displacement, velocity, and acceleration of each story level, for 16 earthquake accelerograms of Table 1 are evaluated, the results of only 7 of which, for brevity, are presented in Table 2. Moreover, the average values of the maximum responses corresponding to all 16 accelerograms are also provided in the last row of Table 2. These results will be used for comparison with the controlled responses by the proposed control devices in the next sections.

6. Design of Tuned Mass Damper (TMD) system

The Tuned Mass Damper (TMD) system is a well-accepted control device used to reduce structural vibrations due to environmental dynamic loadings, such as earthquake excitations. This system includes a mass, spring and damper; and

can be installed on the roof of the building for reducing the seismic responses of the building by both changing its dynamic properties and increasing its damping. In high rise buildings, the dominant mode is often the first mode of the vibration and, therefore, the TMD system is tuned to this mode. In this system, determination of its main parameters, such as the mass, stiffness and damping ratio of the system, is very important and, in the present research study, these parameters are explained in Eqs. (18)–(20). In this study, in order to optimally design the TMD system using the multi-objective optimization procedure, by noting the fact, on the one hand, that the tuning frequency should be close to the fundamental frequency of the structure [44], and, from a practical point of view, that providing large values of mass and damping ratio is difficult, the variation domains of its main parameters are chosen, as shown in Table 3.

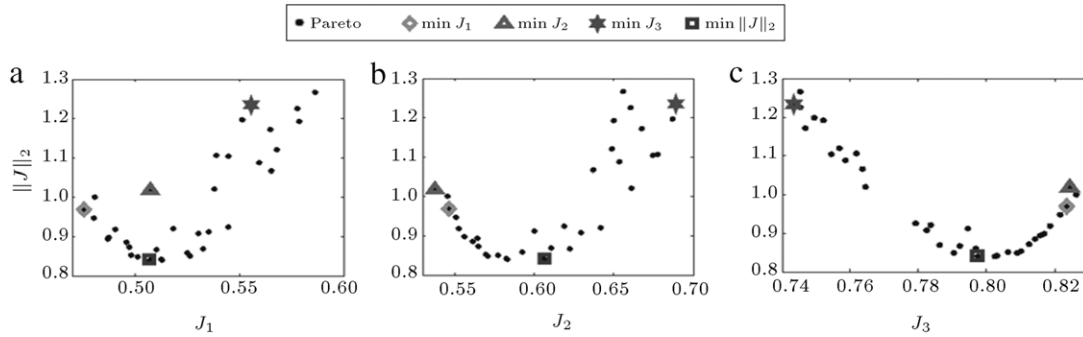


Figure 3: 2-norm level diagrams of Pareto front of the TMD for Coalinga earthquake: (a) J_1 ; (b) J_2 ; and (c) J_3 .

Table 3: Variation domains of the TMD main parameters.

TMD parameters	Minimum value	Maximum value
m_0	1%	3%
β	0.8	1.3
ξ_{TMD}	5%	40%

6.1. Optimal design of the TMD system

In order to achieve the best performance of the control device, the main parameters of the TMD should be optimally designed. In this study, multi-objective optimization is used to determine the optimum values of these parameters, using genetic algorithms. For this purpose, three non-commensurable objective functions, namely, maximum displacement, maximum velocity and maximum acceleration, of each floor of the building are considered, which are minimized simultaneously by multi-objective optimization. These objective functions can be expressed as the following:

$$\begin{aligned}
 J_1 &= \max_i [\max_t |D_i^c(t)| / \max_t |D_i^{uc}(t)|], \\
 J_2 &= \max_i [\max_t |V_i^c(t)| / \max_t |V_i^{uc}(t)|], \\
 J_3 &= \max_i [\max_t |A_i^c(t)| / \max_t |A_i^{uc}(t)|]
 \end{aligned}
 \tag{28}$$

where $i = 1, \dots, 12$ indicate the number of floors of the building, and $D_i^c(t)$, $D_i^{uc}(t)$, $V_i^c(t)$, $V_i^{uc}(t)$, $A_i^c(t)$ and $A_i^{uc}(t)$ are the displacement, velocity and acceleration of each floor of the building in controlled and uncontrolled cases, respectively.

It should be noted that it is impossible to illustrate the trade-off point when more than two objective functions are considered. To overcome to this problem, several multi-dimensional visualization methods are proposed in the literature. One of these methods, which leads to comprehensive analysis of the Pareto front and is called the *Level Diagrams* method [45], is used here to visualize the Pareto fronts of the multi-objective optimization. In this method, each point of the Pareto front must be normalized to bring it between 0 and 1, based on its minimum and maximum values, as [45]:

$$\begin{aligned}
 J_i^M &= \max J_i, & J_i^m &= \min J_i, & i &= 1, 2, 3 \\
 \bar{J}_i &= \frac{J_i - J_i^m}{J_i^M - J_i^m}.
 \end{aligned}
 \tag{29}$$

The distance of each Pareto front point from its origin can be used for comparison. Here, the Euclidean norm of all

objective functions ($\|\bar{J}\|_2 = \sqrt{\sum_{i=1}^3 \bar{J}_i^2}$) is used for this purpose. To represent the Pareto front, the Y axis is specified for the Euclidean norm of all objective functions and the X axis is specified for each objective function. Therefore, each objective function has its own graphical representation, whilst the Y axis of all graphs would be the same.

In this study, multi-objective optimization is used to evaluate the optimal values of the parameters of the TMD system for all 16 reference accelerograms, from which, for brevity, only the Pareto fronts for the Coalinga earthquake are shown in Figure 3.

It is obvious from Figure 3(a) that the point with the lowest value of J_1 has the high value of objective function, J_3 (Figure 3(c)), this issue is true regarding the point with the lowest value of J_3 in comparison to its value for J_1 , so there is a conflict between J_1 and J_3 . Likewise, there is confliction between J_2 and J_3 . As a result, three objective functions are in conflict with each other. This subject shows the Pareto concept. Therefore, a selected point with the lowest value of $\|\bar{J}\|_2$ is a good compromise point, because it has the intermediate value of the three objective functions, so, all results are presented for this point. The optimized controlled responses of the building at each story level (corresponding to the point having the lowest value of $\|\bar{J}\|_2$) for 7 selected accelerograms are presented in Table 4. Moreover, in last row of the table, the average values of these responses for all 16 reference accelerograms are given, which can be used for comparison with the uncontrolled responses.

It can be seen from Table 4 that the average values of the maximum displacement, velocity and acceleration of the building's top story with the TMD system, in comparison with uncontrolled ones, have been approximately reduced to about 30%, 30%, and 17%, respectively.

Furthermore, the values of the TMD parameters and the corresponding objective function values for the optimum point with the lowest value of $\|\bar{J}\|_2$ for 16 earthquake excitations are given in Table 5. It is seen from the table that the average optimal values of the parameters, m_0 , β , and ξ_{TMD} , are obtained as 2.93%, 1.02%, and 10.73%, respectively.

Moreover, Figure 4 compares the time histories of the controlled and uncontrolled responses of the building's top story for the Coalinga earthquake and for the optimum point with the lowest value of $\|\bar{J}\|_2$. This figure also shows that the designed TMD system appropriately controls the building's seismic responses.

In the optimal design procedure of the TMD system, the optimal values of its parameters are being calculated for each reference accelerogram separately. Since the TMD system is a kind of passive control device, its parameters are constant

Table 4: Stories responses with TMD system (Dis = displacement (cm), Vel = velocity (m/s) and Acc = acceleration (m/s²)).

Earthquakes		Stories of the building											
		1st	2nd	3rd	4th	5th	6th	7th	8th	9th	10th	11th	12th
Kobe	Dis	0.18	0.81	1.20	1.62	2.05	2.51	2.99	3.51	4.03	4.56	5.07	5.62
	Vel	0.01	0.04	0.05	0.07	0.09	0.11	0.13	0.16	0.18	0.20	0.23	0.25
	Acc	0.05	0.22	0.33	0.45	0.57	0.70	0.83	0.98	1.12	1.27	1.42	1.57
Kocaeli	Dis	0.55	2.46	3.67	4.94	6.26	7.65	9.11	10.65	12.20	13.73	15.26	16.83
	Vel	0.02	0.11	0.16	0.21	0.27	0.33	0.39	0.45	0.52	0.59	0.65	0.72
	Acc	0.13	0.56	0.84	1.13	1.42	1.73	2.07	2.42	2.77	3.11	3.45	3.81
Chi-Chi	Dis	0.20	0.88	1.31	1.76	2.23	2.73	3.26	3.81	4.38	4.95	5.51	6.10
	Vel	0.01	0.04	0.06	0.09	0.11	0.13	0.16	0.19	0.21	0.24	0.27	0.30
	Acc	0.07	0.33	0.49	0.66	0.83	1.02	1.21	1.42	1.63	1.83	2.04	2.25
Morgan hill	Dis	0.16	0.70	1.04	1.40	1.78	2.18	2.59	3.03	3.48	3.93	4.37	4.83
	Vel	0.01	0.03	0.05	0.07	0.08	0.10	0.12	0.14	0.16	0.19	0.21	0.23
	Acc	0.08	0.34	0.50	0.67	0.86	1.05	1.25	1.46	1.68	1.91	2.12	2.35
San Fernando	Dis	0.08	0.38	0.56	0.75	0.96	1.17	1.39	1.63	1.88	2.13	2.37	2.63
	Vel	0.00	0.02	0.03	0.03	0.04	0.05	0.06	0.07	0.09	0.10	0.11	0.12
	Acc	0.04	0.19	0.28	0.38	0.48	0.59	0.70	0.82	0.94	1.06	1.18	1.30
Northridge	Dis	0.24	1.08	1.60	2.16	2.74	3.35	3.99	4.68	5.38	6.08	6.78	7.50
	Vel	0.01	0.05	0.07	0.09	0.12	0.15	0.17	0.21	0.24	0.27	0.30	0.33
	Acc	0.06	0.29	0.43	0.58	0.73	0.90	1.07	1.25	1.44	1.62	1.81	2.00
Coalinga	Dis	0.28	1.23	1.84	2.47	3.13	3.83	4.56	5.34	6.13	6.93	7.71	8.53
	Vel	0.01	0.06	0.09	0.12	0.15	0.19	0.22	0.26	0.30	0.34	0.38	0.42
	Acc	0.10	0.43	0.64	0.87	1.10	1.34	1.60	1.87	2.14	2.40	2.67	2.94
Average responses	Dis	0.24	1.09	1.62	2.18	2.77	3.38	4.03	4.72	5.41	6.11	6.81	7.53
	Vel	0.01	0.05	0.07	0.09	0.12	0.14	0.17	0.20	0.23	0.26	0.29	0.32
	Acc	0.08	0.34	0.50	0.68	0.86	1.05	1.25	1.47	1.69	1.90	2.12	2.34

Table 5: Optimum values of the TMD design parameters for different earthquake excitations.

Earthquakes	Design parameters and objective functions						
	m_0	β	ξ_{TMD}	J_1	J_2	J_3	$\ U\ _2$
Kobe	3	0.82	5.3	0.53	0.51	0.62	0.54
Cape Mendocino	3	1.22	5.1	0.75	0.68	0.63	0.51
Chi-Chi	2.8	0.84	12	0.58	0.65	0.95	0.67
Imperial valley	2.45	0.99	28	0.85	0.95	1.01	0.66
Kocaeli	3	1.05	7.5	0.71	0.65	0.71	0.77
Northridge	2.78	0.95	9	0.76	0.83	0.81	0.72
Landers	3	0.86	10.4	0.83	0.74	0.87	0.76
Morgan hill	3	1.02	6	0.78	0.77	0.85	0.49
San Fernando	3	1.11	9.8	0.71	0.78	0.96	0.82
Coalinga	3	1.05	5.6	0.51	0.61	0.80	0.84
Duze	3	0.89	5.1	0.65	0.70	0.86	0.60
Whittler narrows	3	1.30	15	0.85	0.86	0.97	0.67
Bam	3	1.012	10.41	0.84	0.92	0.90	0.50
Zanjiran	3	1.05	28.8	0.71	0.77	0.96	0.68
Garmkhan	2.92	1.15	8.6	0.80	0.60	0.78	0.68
Karebas	3	0.99	5	0.82	0.75	0.88	0.54
Average	2.93	1.02	10.73	–	–	–	–

during its lifetime. Consequently, the final decision about the optimal values of the design parameters must be made, based on the different values obtained for separate accelerograms. For this purpose, three methods, explained in the following, are used to obtain the optimal value of any design parameter:

- I. The expected mean value calculated for reference accelerograms: $E(x) = \frac{\sum x_i}{n}$, where $E(x)$ is the expected mean value of parameter x ; x_i is the optimal value of the parameter obtained for each accelerogram; and n is the number of total accelerograms.
- II. The expected mean value + one standard deviation ($\sigma(x)$): $E(x) + 1\sigma(x)$.
- III. The weighted mean value, for which, the reduction ratio of controlled and uncontrolled displacements is taken as the weighting coefficient.

Table 6: TMD design parameters obtained from the proposed three methods.

Different methods	TMD parameters		
	m_0	β	ξ_{TMD}
First method	2.93	1.02	10.73
Second method	3.08	1.15	17.96
Third method	2.94	1	9.91

The results of optimal values of the TMD design parameters, calculated by applying these three methods, are shown in Table 6.

In order to select the final values for the TMD parameters among these three groups, the building is analyzed with these TMDs, and the average values of maximum displacement,

Table 7: Average values of the maximum controlled responses of the building for three proposed methods (D_{\max} = maximum average displacement (cm), V_{\max} = maximum average velocity (m/s) and a_{\max} = maximum average acceleration (m/s^2)).

		Stories of the building											
		1st	2nd	3rd	4th	5th	6th	7th	8th	9th	10th	11th	12th
The first method		TMD parameters $m_0 = 2.93\%$, $\beta = 1.02$, $\xi_{\text{TMD}} = 10.73\%$											
Average values	D_{\max}	0.27	1.22	1.81	2.43	3.08	3.77	4.50	5.27	6.05	6.84	7.62	8.43
	V_{\max}	0.01	0.05	0.08	0.11	0.13	0.16	0.19	0.23	0.26	0.29	0.33	0.36
	a_{\max}	0.08	0.36	0.53	0.71	0.90	1.10	1.31	1.54	1.76	1.99	2.21	2.44
The second method		TMD parameters $m_0 = 3.08\%$, $\beta = 1.15$, $\xi_{\text{TMD}} = 17.96\%$											
Average values	D_{\max}	0.29	1.29	1.91	2.57	3.27	4.00	4.76	5.58	6.41	7.24	8.05	8.91
	V_{\max}	0.01	0.05	0.08	0.11	0.14	0.17	0.20	0.23	0.26	0.30	0.33	0.37
	a_{\max}	0.08	0.35	0.53	0.71	0.90	1.10	1.31	1.53	1.76	1.98	2.21	2.44
The third method		TMD parameters $m_0 = 2.94\%$, $\beta = 1.00$, $\xi_{\text{TMD}} = 9.91\%$											
Average values	D_{\max}	0.27	1.20	1.79	2.40	3.05	3.73	4.44	5.20	5.98	6.76	7.53	8.33
	V_{\max}	0.01	0.05	0.08	0.10	0.13	0.16	0.19	0.23	0.26	0.29	0.32	0.36
	a_{\max}	0.08	0.36	0.53	0.71	0.91	1.11	1.32	1.54	1.77	1.99	2.22	2.45

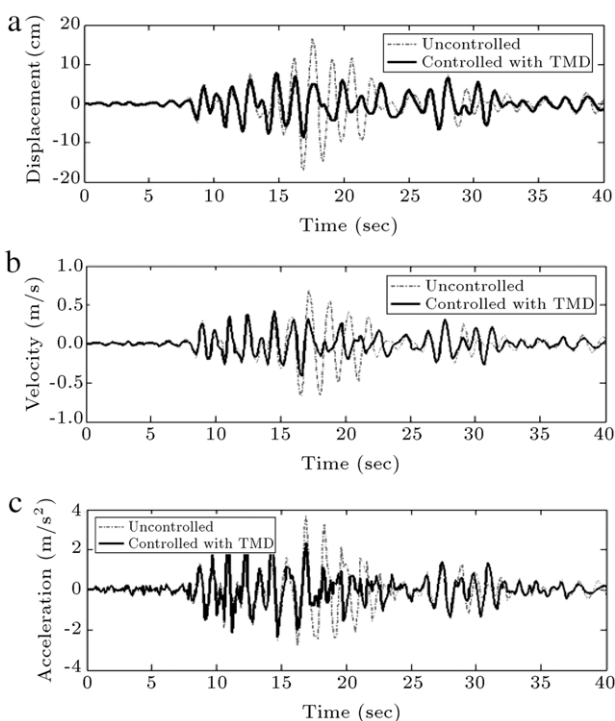


Figure 4: Comparison of the controlled and uncontrolled responses of the building top story for Coalinga earthquake: (a) displacement; (b) velocity; and (c) acceleration.

velocity and acceleration of each story level for 16 reference earthquake accelerograms are calculated and presented in Table 7.

By comparing the results given in the table, it can be concluded that the third method is more appropriate to determine the TMD design parameters, in which the resulting parameters give more reduction in structural response. Consequently, the final values of the TMD design parameters are proposed as: $m_0 = 2.94\%$, $\beta = 1$, $\xi_{\text{TMD}} = 9.91\%$.

According to Table 7, the results obtained from the third method show reduction ratios of about 21.3%, 21% and 12.3% for maximum values of displacement, velocity and acceleration of the building's top story, respectively.

6.2. Robust design of TMD with uncertain parameters

The dynamic behavior of a building is dependent on its natural frequencies and mode shapes. Moreover, the damping of the structure plays an important role in reducing the seismic responses of the building. These two are the most important parameters of structures that could be affected by different sources. Therefore, in this study, it is assumed that the stiffness matrix and the structural damping ratio of the building may be different from those considered in deterministic analyses, and, thus, these parameters should be treated as uncertain by assuming pre-defined probabilistic distributions. Consequently, in order to minimize the performance degradation of the control system from its ideal deterministic position, the uncertainties that may exist in these parameters must be taken into account through a stochastic Robust Design Optimization (RDO) approach. The control system which is designed by the stochastic robust optimization approach is then less sensitive to random variations of uncertain parameters. As mentioned earlier, in the stochastic robust design approach, it is necessary to assume probabilistic distributions for uncertain parameters.

There are many probability distribution functions representing a variety of conditions. In this study, the well known standard Beta distribution with shape coefficients $a = b = 2$ has been used, for which the PDF is expressed as [41]:

$$f(x|a, b) = \frac{1}{B(a, b)} x^{a-1} (1-x)^{b-1} I_{(0,1)}(x), \quad (30)$$

where $B(\cdot)$ is the Beta function, and the indicator function, $I_{(0,1)}(x)$, ensures that only the values of x in the range $(0, 1)$ have nonzero probability. This Beta distribution function is shown in Figure 5.

In this research study, in order to perform the stochastic RDO procedure, the stiffness and damping ratios of the building are considered uncertain random variables with maximum $\pm 20\%$ variation around their nominal values. For accomplishment of this procedure, the building uncertain stiffness matrix, $[K_u]$, and that of the damping ratio, ξ_u , are defined as the following:

$$[K_u] = \alpha_1 [K], \quad (31a)$$

and:

$$\xi_u = \alpha_2 \xi, \quad (31b)$$

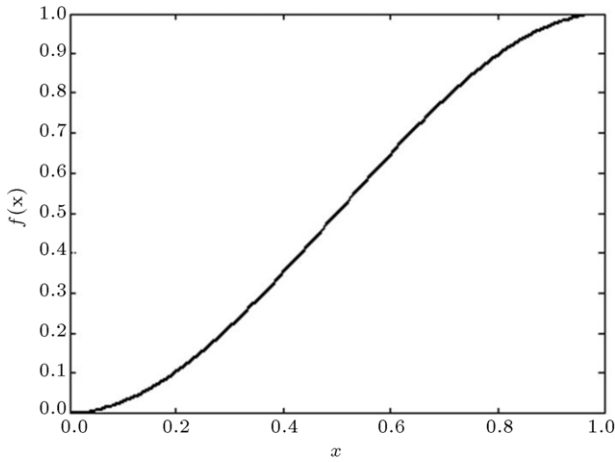


Figure 5: Beta distribution function.

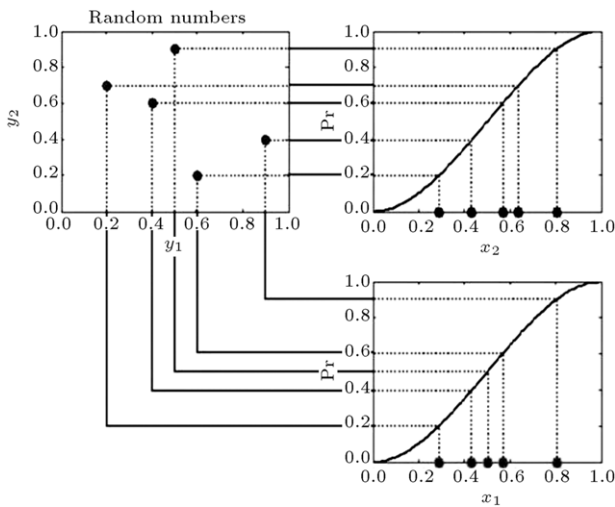


Figure 6: Hammersley method of simulation.

where $[K]$ and ξ are the deterministic values of the stiffness matrix and damping ratio of the building, respectively, and the uncertainty coefficients, α_1 and α_2 , with mean values of 1 and Coefficient Of Variations (COV) of $\pm 20\%$, are considered to incorporate the uncertainties that exist in $[K]$ and ξ . Coefficients α_1 and α_2 follow the probabilistic beta distribution given in Eq. (30). It is noted that in Eq. (30), the value x varies between 0 and 1, while the uncertainty coefficients, α_1 and α_2 , vary between 0.8 and 1.2. This incompatibility is accomplished through the computer programming procedure. In this study, the Hammersley Sequence Sampling (HSS) is used to simulate the probabilistic behavior of the building. The advantage of this method in comparison with the Monte Carlo method is that, in this method, a specified pattern with uniform distribution is used to generate the random numbers between 0 and 1. Therefore, better results can be achieved with fewer samples [42]. This simulation and mapping procedure are depicted in Figure 6, when uncertain variable, x , varies between 0 and 1, following standard beta distribution. In this figure, y_1 and y_2 are the random numbers uniformly distributed between 0 and 1.

In the present study, to perform the stochastic RDO procedure using the HSS approach, 50 pairs of uniformly distributed numbers are simulated between 0 and 1, by which, 50 pairs of random uncertainty coefficients, α_1 and α_2 , are

simulated through a similar mapping procedure, shown in Figure 6, by considering a beta distribution for these two variables. Then, using these 50 pairs of coefficients, α_1 and α_2 , 50 pairs of uncertain stiffness matrix $[K_u]$ and damping ratio, ξ_u , are simulated, resulting in 50 buildings with different stiffness matrices and damping ratios. Now, these 50 buildings are analyzed under the application of 16 reference earthquake accelerograms given in Table 1. The average values of the maximum responses of these buildings, including maximum displacement, velocity, and acceleration of each story level, for 7 accelerograms, are provided in Table 8. These results will be used for comparison with the controlled responses of the robust TMD system in the next sections.

In order to stochastic robust design optimization of the TMD system, three objective functions are defined as follows:

$$J_1 = \frac{E(\max_i[\max_t |D_i^c(t)| / \max_t |D_i^{uc}(t)|])}{\sigma^2(\max_i[\max_t |D_i^c(t)| / \max_t |D_i^{uc}(t)|]) + \frac{E_{01}}{\sigma_{01}^2}}, \quad (32a)$$

$$J_2 = \frac{E(\max_i[\max_t |V_i^c(t)| / \max_t |V_i^{uc}(t)|])}{\sigma^2(\max_i[\max_t |V_i^c(t)| / \max_t |V_i^{uc}(t)|]) + \frac{E_{02}}{\sigma_{02}^2}}, \quad (32b)$$

$$J_3 = \frac{E(\max_i[\max_t |A_i^c(t)| / \max_t |A_i^{uc}(t)|])}{\sigma^2(\max_i[\max_t |A_i^c(t)| / \max_t |A_i^{uc}(t)|]) + \frac{E_{03}}{\sigma_{03}^2}}, \quad (32c)$$

where E_{0i} and σ_{0i}^2 are the desired mean and variance of each stochastic response, respectively, which can be chosen by the designer. For example, for the Coalinga earthquake, the values of the deterministic objective functions for the trade-off point (the point with the lowest $\|J\|_2$) are considered as E_{0i} values, which are, as follows: $E_{01} = 0.51$, $E_{02} = 0.61$, $E_{03} = 0.8$. Furthermore, in order to have the minimum variation, the values of σ_{0i}^2 are considered as 0.001. In the multi-objective optimization process, using the NSGA-II approach, the above three objective functions should be simultaneously minimized to get the perfect performance of the control system. Similar to the previous sections, the Pareto fronts for the Coalinga earthquake are shown in Figure 7 for the robust TMD system. It can be seen from the figure that there is a conflict between J_1 and J_3 . It means that the TMD system with lower displacement has higher acceleration. The same conflict can be found in Figure 7, between J_2 and J_3 . The squared point in the Pareto front, which has the lowest value of the 2-norm of the Level Diagram, has the low value of each objective function. Therefore, it can be considered an outstanding optimum point. For this optimum point, the mean and variance of each stochastic response and the values of the TMD design parameters obtained for the Coalinga earthquake are given in Table 9.

The average values of the optimized stochastic responses of the 50 buildings simulated for the robust design of the TMD system (corresponding to the point having the lowest value of $\|J\|_2$) are presented in Table 10 at each story level for each of the 7 considered accelerograms. Moreover, in the last row of the table the ensemble average values of these responses for the 16 reference accelerograms are given, which

Table 8: Average values of the stories maximum responses corresponding to 50 simulated buildings (Dis = displacement (cm), Vel = velocity (m/s) and Acc = acceleration (m/s^2)).

Earthquakes		Stories of the building											
		1st	2nd	3rd	4th	5th	6th	7th	8th	9th	10th	11th	12th
Kobe	Dis	0.38	1.70	2.52	3.40	4.31	5.28	6.29	7.37	8.47	9.57	10.65	11.79
	Vel	0.02	0.07	0.11	0.14	0.18	0.22	0.27	0.31	0.36	0.41	0.45	0.50
	Acc	0.08	0.35	0.52	0.70	0.89	1.09	1.30	1.52	1.76	1.99	2.22	2.47
Cape Mendocino	Dis	0.50	2.23	3.31	4.46	5.66	6.93	8.25	9.67	11.11	12.55	13.97	15.45
	Vel	0.02	0.08	0.13	0.17	0.21	0.26	0.31	0.37	0.42	0.48	0.53	0.59
	Acc	0.08	0.36	0.54	0.73	0.92	1.12	1.34	1.56	1.79	2.02	2.24	2.47
Whittler Narrows	Dis	0.09	0.41	0.61	0.82	1.04	1.27	1.51	1.77	2.03	2.30	2.55	2.82
	Vel	0.00	0.02	0.03	0.04	0.05	0.06	0.07	0.08	0.09	0.10	0.11	0.13
	Acc	0.06	0.29	0.42	0.57	0.72	0.89	1.06	1.24	1.42	1.60	1.78	1.97
Morgan Hill	Dis	0.22	0.98	1.46	1.97	2.49	3.05	3.63	4.25	4.88	5.51	6.14	6.78
	Vel	0.01	0.04	0.07	0.09	0.11	0.14	0.16	0.19	0.22	0.25	0.28	0.30
	Acc	0.09	0.39	0.57	0.77	0.98	1.20	1.43	1.68	1.93	2.19	2.44	2.70
San Fernando	Dis	0.12	0.53	0.79	1.07	1.35	1.66	1.97	2.31	2.66	3.00	3.34	3.69
	Vel	0.01	0.02	0.03	0.05	0.06	0.07	0.08	0.10	0.11	0.13	0.14	0.16
	Acc	0.04	0.20	0.29	0.39	0.50	0.61	0.72	0.84	0.97	1.09	1.22	1.34
Northridge	Dis	0.35	1.57	2.34	3.15	4.00	4.90	5.83	6.83	7.84	8.86	9.86	10.90
	Vel	0.01	0.07	0.10	0.13	0.17	0.20	0.24	0.28	0.32	0.37	0.41	0.45
	Acc	0.08	0.34	0.50	0.67	0.86	1.05	1.25	1.46	1.68	1.89	2.11	2.33
Coalinga	Dis	0.52	2.30	3.43	4.62	5.85	7.16	8.53	10.00	11.49	13.00	14.47	16.02
	Vel	0.02	0.10	0.15	0.20	0.25	0.30	0.36	0.42	0.49	0.55	0.61	0.68
	Acc	0.11	0.51	0.75	1.01	1.28	1.57	1.87	2.19	2.51	2.83	3.14	3.47
Average responses	Dis	0.31	1.39	2.07	2.78	3.53	4.32	5.14	6.03	6.93	7.83	8.71	9.64
	Vel	0.01	0.06	0.09	0.12	0.15	0.18	0.21	0.25	0.29	0.33	0.36	0.40
	Acc	0.08	0.35	0.51	0.69	0.88	1.08	1.28	1.50	1.72	1.94	2.16	2.39

Table 9: Parameters of the selected optimum point obtained for Coalinga earthquake.

m_0	β	ξ_{TMD}	E_1	σ_1^2	E_2	σ_2^2	E_3	σ_3^2
2.94%	0.94	5.41%	0.5731	$5e-4$	0.6226	$1.9e-3$	0.8158	$7e-4$

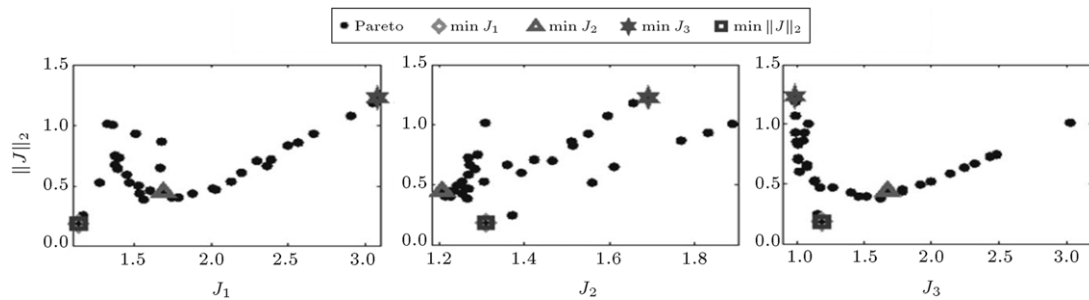


Figure 7: 2-norm level diagrams of Pareto front of the robust TMD for Coalinga earthquake.

can be used for comparison with those of the uncontrolled ones. It can be seen from the table that the average values of stochastic displacement, velocity, and acceleration of the building's top story, obtained from robust design of the TMD system, in comparison with those of the uncontrolled ones, are approximately reduced to about 34.02%, 32.5% and 15.48%, respectively.

Furthermore, the values of the design parameters of the TMD device evaluated during the RDO procedure of this system, and the corresponding objective function values for the optimum point with the lowest value of $\|J\|_2$ for 7 earthquake excitations are presented in Table 11. It is seen from the table that the stochastic average optimal values of the design parameters, m_0 , β and ξ_{TMD} , are obtained as 2.87%, 1, and 10.2%, respectively,

while, from deterministic analysis, these values are obtained about 2.93%, 1.02, and 10.73%, respectively.

Moreover, Figure 8 compares the time histories of the robust controlled and uncontrolled responses of the building's top story for the Coalinga earthquake for the optimum point with the lowest value of $\|J\|_2$. This figure also shows that the robust design of the TMD system is an appropriate procedure to control the seismic responses of the building.

The stochastic time history responses of the building's top floor for the above mentioned optimum robustly designed TMD system is shown in Figure 9. In this figure, the dashed lines show the stochastic responses of the building's top floor calculated for 50 simulated sample buildings, and the solid line shows the mean values of these responses.

Table 10: Average values of the optimized stochastic responses of the buildings simulated for the robust design of the TMD system (Dis = displacement (cm), Vel = velocity (m/s) and Acc = acceleration (m/s^2)).

Earthquakes		Stories of the building											
		1st	2nd	3rd	4th	5th	6th	7th	8th	9th	10th	11th	12th
Kobe	Dis	0.18	0.82	1.21	1.63	2.07	2.54	3.03	3.55	4.08	4.62	5.14	5.69
	Vel	0.01	0.04	0.05	0.07	0.09	0.11	0.14	0.16	0.18	0.21	0.23	0.25
	Acc	0.06	0.25	0.36	0.49	0.62	0.76	0.91	1.07	1.23	1.40	1.56	1.73
Cape Mendocino	Dis	0.39	1.72	2.56	3.45	4.38	5.36	6.39	7.48	8.59	9.71	10.81	11.95
	Vel	0.01	0.06	0.09	0.12	0.15	0.19	0.22	0.26	0.30	0.34	0.38	0.42
	Acc	0.06	0.25	0.38	0.51	0.64	0.78	0.93	1.09	1.24	1.39	1.55	1.70
Whittler Narrows	Dis	0.08	0.36	0.54	0.73	0.92	1.13	1.34	1.57	1.80	2.03	2.26	2.50
	Vel	0.00	0.02	0.02	0.03	0.04	0.05	0.06	0.07	0.08	0.09	0.10	0.11
	Acc	0.06	0.28	0.42	0.56	0.71	0.87	1.04	1.21	1.39	1.57	1.74	1.93
Morgan Hill	Dis	0.17	0.76	1.13	1.51	1.92	2.34	2.79	3.27	3.75	4.24	4.72	5.22
	Vel	0.01	0.03	0.05	0.07	0.08	0.10	0.12	0.14	0.16	0.19	0.21	0.23
	Acc	0.08	0.34	0.50	0.67	0.85	1.05	1.25	1.46	1.68	1.90	2.12	2.35
San Fernando	Dis	0.09	0.40	0.59	0.80	1.02	1.24	1.48	1.73	1.99	2.25	2.51	2.78
	Vel	0.00	0.02	0.03	0.04	0.05	0.06	0.07	0.08	0.09	0.10	0.12	0.13
	Acc	0.04	0.20	0.29	0.39	0.50	0.61	0.72	0.85	0.97	1.10	1.22	1.35
Northridge	Dis	0.22	0.98	1.46	1.96	2.49	3.05	3.64	4.27	4.92	5.57	6.22	6.90
	Vel	0.01	0.05	0.07	0.10	0.12	0.15	0.18	0.21	0.24	0.27	0.30	0.33
	Acc	0.07	0.29	0.43	0.59	0.74	0.91	1.08	1.27	1.46	1.65	1.84	2.03
Coalinga	Dis	0.31	1.38	2.05	2.76	3.50	4.28	5.09	5.96	6.84	7.71	8.58	9.48
	Vel	0.01	0.06	0.09	0.13	0.16	0.19	0.23	0.27	0.31	0.35	0.39	0.43
	Acc	0.10	0.44	0.66	0.89	1.13	1.38	1.64	1.92	2.20	2.48	2.75	3.03
Average responses	Dis	0.21	0.92	1.36	1.83	2.33	2.85	3.39	3.98	4.57	5.16	5.75	6.36
	Vel	0.01	0.04	0.06	0.08	0.10	0.12	0.15	0.17	0.19	0.22	0.25	0.27
	Acc	0.07	0.29	0.43	0.59	0.74	0.91	1.08	1.27	1.45	1.64	1.83	2.02

Table 11: Stochastic optimum values of the TMD design parameters for different earthquake excitations.

Earthquakes	The values of design parameters and objective functions						
	m_0	β	ξ_{TMD}	J_1	J_2	J_3	$\ J\ _2$
Kobe	2.98	0.80	5.53	1.61	1.16	1.41	0.35
Cape Mendocino	2.72	1.20	5.94	1.26	1.07	1.29	0.48
Northridge	2.65	0.87	15.56	1.10	1.09	1.13	0.62
Morgan Hill	2.97	1.05	8.91	1.27	1.71	1.32	0.55
San Fernando	2.98	0.87	7.24	1.22	1.22	1.08	0.64
Coalinga	2.94	0.94	5.41	1.14	1.31	1.18	0.19
Whittler Narrows	2.83	1.27	22.8	1.54	1.73	1.31	0.40
Average	2.87	1.00	10.2	–	–	–	–

Table 12: Robust TMD design parameters obtained from the proposed three averaging methods.

TMD parameters	m_0	β	ξ_{TMD}
First method	2.87	1.00	10.20
Second method	2.99	1.17	16.30
Third method	2.83	0.932	10.03

It is evident from Figure 9 that all the individual stochastic responses corresponding to 50 sample buildings and their mean values, are very close to each other. It means that the robust design of the control system significantly reduces the effect of uncertainties existing in the structure, leading to a control system with less sensitivity to the uncertainties of the system.

Here, also, the same three averaging methods explained earlier are used to determine the final values of the robust TMD design parameters. The results obtained for TMD design parameters in this way are shown in Table 12. In order to select the final values for the robust TMD design parameters among these three groups, the building is analyzed by considering these values for TMD parameters, and the average values of the maximum displacement, velocity, and acceleration of

each story level for 16 reference earthquake accelerograms are calculated and presented in Table 13. By comparing the results given in the table, it can be concluded that the third method is more appropriate to determine the design parameters of the robust TMD system, in which the resulting parameters give more reduction in structural responses. Consequently, the final values of the design parameters for the robust TMD system are proposed as: $m_0 = 2.83\%$, $\beta = 0.932$, $\xi_{TMD} = 10.03\%$. According to Table 13, the results obtained from the third method show reduction ratios about 27.6%, 25% and 12.13% on maximum values of displacement, velocity, and acceleration of the building's top story, respectively, while these reduction ratios, obtained from deterministic analysis, are about 21.13%, 21%, and 12.3%, respectively.

In order to compare the results of deterministic and robust design optimization methods, the 50 sample buildings simulated in previous sections are analyzed by considering the optimal values of the TMD design parameters (m_0 , β , and ξ_{TMD}) obtained from these two methods. For this purpose, 50 sample buildings are analyzed by considering the optimal TMD system for the trade-off point (the point with the minimum value of $\|J\|_2$) in each earthquake excitation, and the results of analysis

Table 13: Average values of the maximum stochastic responses of the building for three methods (D_{\max} = maximum average displacement (cm), V_{\max} = maximum average velocity (m/s) and a_{\max} = maximum average acceleration (m/s^2)).

		Stories of the building											
		1st	2nd	3rd	4th	5th	6th	7th	8th	9th	10th	11th	12th
The first method		$m_0 = 2.87\%, \beta = 1.00, \xi_{TMD} = 10.2\%$											
Average values	D_{\max}	0.23	1.02	1.51	2.04	2.58	3.16	3.76	4.41	5.07	5.72	6.37	7.05
	V_{\max}	0.01	0.04	0.06	0.09	0.11	0.13	0.16	0.19	0.21	0.24	0.27	0.30
	a_{\max}	0.07	0.30	0.45	0.61	0.77	0.94	1.12	1.31	1.50	1.70	1.89	2.08
The second method		$m_0 = 2.99\%, \beta = 1.17, \xi_{TMD} = 16.3\%$											
Average values	D_{\max}	0.25	1.14	1.69	2.27	2.88	3.53	4.20	4.92	5.66	6.40	7.12	7.88
	V_{\max}	0.01	0.05	0.07	0.09	0.12	0.15	0.17	0.20	0.23	0.26	0.29	0.32
	a_{\max}	0.07	0.30	0.45	0.60	0.76	0.93	1.11	1.30	1.49	1.68	1.87	2.06
The third method		$m_0 = 2.83\%, \beta = 0.932, \xi_{TMD} = 10.03\%$											
Average values	D_{\max}	0.23	1.01	1.50	2.02	2.56	3.13	3.73	4.37	5.02	5.67	6.31	6.98
	V_{\max}	0.01	0.04	0.06	0.09	0.11	0.13	0.16	0.18	0.21	0.24	0.27	0.30
	a_{\max}	0.07	0.31	0.45	0.61	0.78	0.95	1.13	1.32	1.52	1.71	1.90	2.10

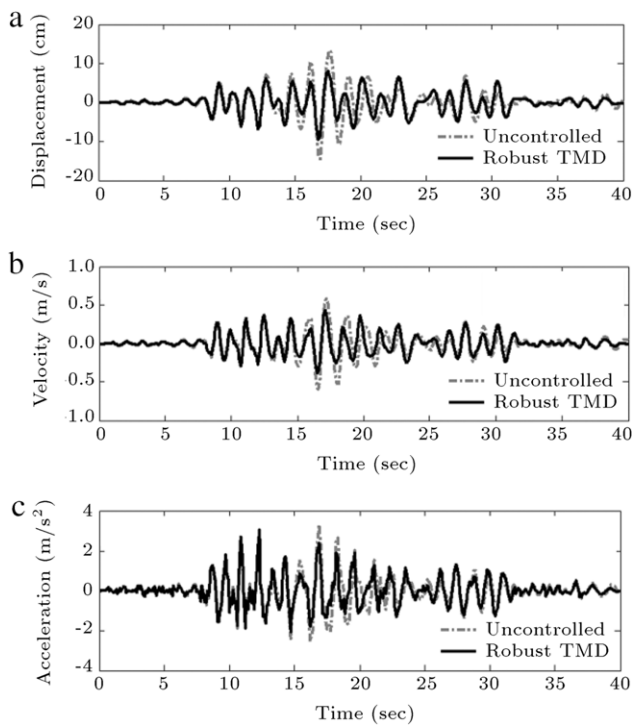


Figure 8: Comparison of the robust controlled and uncontrolled responses of the building top story for Coalinga earthquake: (a) displacement; (b) velocity; and (c) acceleration.

of these 50 samples are taken as the final results for each earthquake excitation. The PDFs of normalized maximum responses of the buildings are shown in Figure 10 for the final optimal TMD design parameters, in the case of robust design, and that of the deterministic design of the TMD system for the Coalinga earthquake. It is clear from the figure that with the robust design of the TMD system, the variation of each objective function from its mean value is very low in comparison with that of the deterministic design, indicating that the robust design is more reliable than the deterministic one.

Moreover, to show the supremacy of the robust design, the variances of the top story responses of the simulated buildings for trade-off points of the robust and deterministic design are shown in Figure 11. It is seen from the figure that the stochastic behavior of the uncertain system can have less variation, if, and only if, the system is designed robustly. Finally, from the above discussion, it is obvious that in order to achieve a safe design, compatible with variations in the parameters and conditions of the system, a robust design would be necessary.

7. Conclusions

In this study, the multi-objective optimization method, using the NSGA-II approach, has been performed to optimally design the TMD control system. Multi-objective optimization of this system led to the discovery of some important trade-offs between the objective functions. Based on the multi-objective GAs of this work, the point which has the lowest value of the Euclidean norm of all objective functions is used

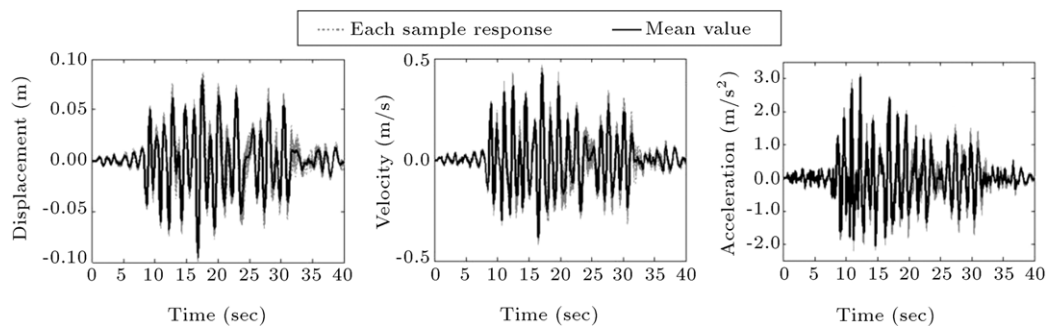


Figure 9: Stochastic response of the top floor for the trade-off point for Coalinga earthquake (dashed lines correspond to each sample response, and the solid line is the mean value of the responses).

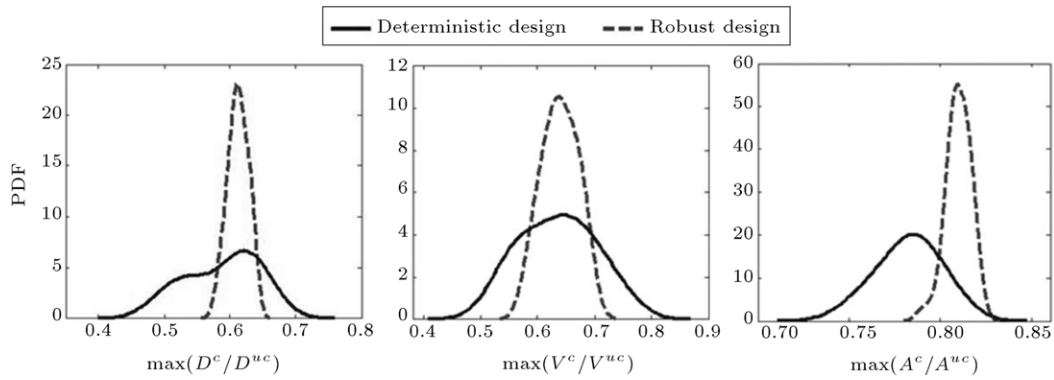


Figure 10: The PDFs of each objective function for Coalinga earthquake.

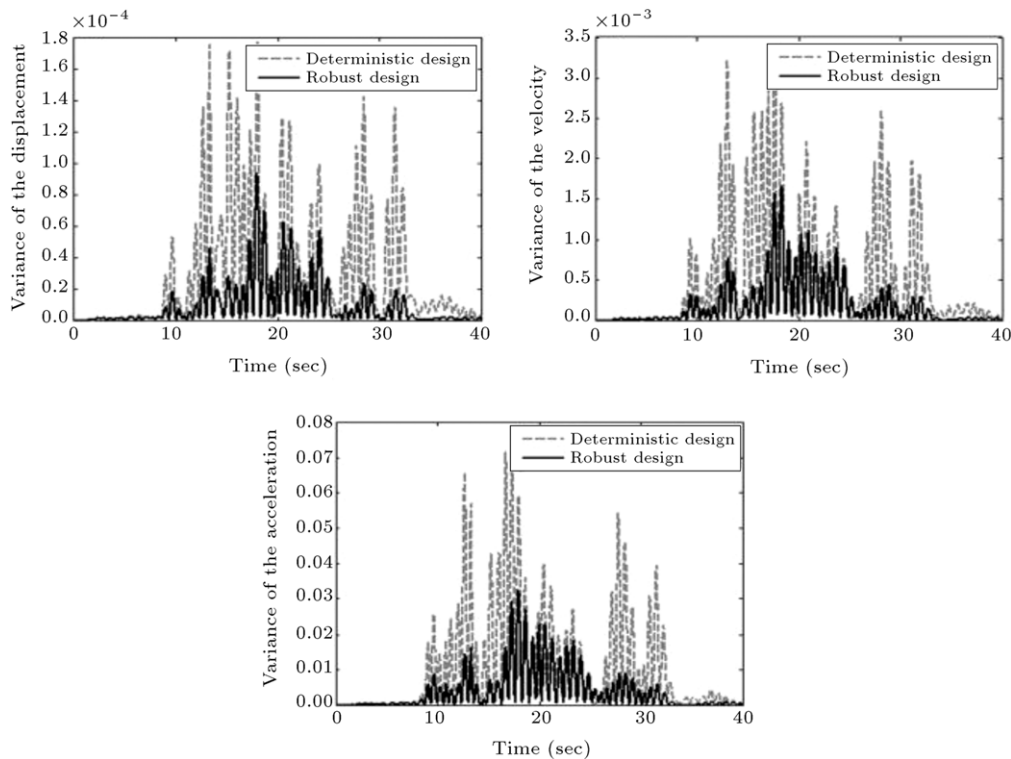


Figure 11: Variance of the stochastic response of the building top floor for Coalinga earthquake.

to compare the application of this device. Moreover, in order to take into account the effects of uncertainties that may exist in the building, a Robust Design Optimization (RDO) procedure is performed. For this purpose, the building stiffness matrix and damping ratio are considered as uncertain parameters. In order to generate sample buildings, the Hammersley Sequence Sampling (HSS) procedure is used. The numerical studies performed in this research work lead to the following conclusions:

1. By performing the deterministic multi-objective optimization procedure, the optimum values of the TMD design parameters are obtained as $m_0 = 2.94\%$, $\beta = 1$, $\xi_{TMD} = 9.91\%$. The results evaluated from simulation show reduction ratios about 21.3%, 21% and 12.3% on the maximum displacement, velocity, and acceleration of the sample building's top story, respectively.
2. By performing the Robust Design Optimization (RDO) procedure, the optimum values of the TMD design parameters are

obtained as $m_0 = 2.83\%$, $\beta = 0.932$, $\xi_{TMD} = 10.03\%$. Applying these values shows reduction ratios about 27.6%, 25% and 12.13% on the maximum displacement, velocity, and acceleration of the building's top story, respectively.

3. It is found that with the robust design of the TMD system, the variation of each objective function from its mean value is very low in comparison with that of the deterministic design, indicating that the robust design is more reliable than the deterministic one.
4. The conflict existing between the objective functions allows the designer to choose the proper point for designing, by establishing a compromise between the objective functions.

References

- [1] Alhan, C. and Gavin, A. "A parametric study of linear and nonlinear passively damped seismic isolation system for buildings", *Engineering Structures*, (24), pp. 485–497 (2004).

- [2] Adhikari, R. and Yamaguchi, H. "Sliding mode control of buildings with ATMD", *Earthquake Engineering and Structural Dynamics*, (26), pp. 409–422 (1997).
- [3] Ahmadi, G. "Overview of base isolation, passive and active vibration control strategies for aseismic design of structures", *Scientia Iranica*, 2(2), pp. 99–116 (1995).
- [4] Hudson, M.J. and Reynolds, P. "Implementation considerations for active vibration control in the design of floor structures", *Engineering Structures*, 44, pp. 334–358 (2012).
- [5] Datta, T.K. "Control of dynamic response of structures", *Proc. of the Indo-US Symposium on Emerging Trends in Vibration and Noise Engineering*, pp. 18–20 (1996).
- [6] Cao, H. and Li, Q.S. "New control strategies for active tuned mass damper systems", *Computers & Structures*, 82, pp. 2341–2350 (2004).
- [7] Ji, H.R., Moon, Y.J., Kim, C.H. and Lee, I.W. "Structural vibration control using semiactive tuned mass damper", *The Eighteenth KCCNN Symposium on Civil Engineering-KAIST6*, Taiwan, pp. 18–20 (2005).
- [8] Soong, T.T. and Dargush, G.F. *Passive Energy Dissipation Systems in Structural Engineering*, John Wiley & Sons Ltd., Baffins Lane, Chichester, England (1997).
- [9] Frahm, H. "Devices for damping vibrations of bodies", *US Patent*, 989, 958 (1911).
- [10] Wang, A. and Lin, Y. "Vibration control of a tall building subjected to earthquake excitation", *Journal of Sound and Vibration*, 299, pp. 757–773 (2007).
- [11] Aldemir, U. "Optimal control of structures with semiactive tuned mass dampers", *Journal of Sound and Vibration*, 266(4), pp. 847–874 (2003).
- [12] Pinkaew, T. and Fujino, Y. "Effectiveness of semi-active tuned mass dampers under harmonic excitation", *Engineering Structures*, 23(7), pp. 850–856 (2001).
- [13] Spencer, B.F. Jr. and Soong, T.T. "New application and development of active, semi-active and hybrid control techniques for seismic and non-seismic vibration in the USA", *Proc. Int. Post-SMIRT Conf. on Seismic Isolation, Passive Energy Dissipation and Active Control of Vibration of Structures*, 1, pp. 467–488 (1999).
- [14] Lee, M.H. "Active control to reduce the horizontal seismic response of buildings taking into account the soil–structure interaction", *Soil Dynamics and Earthquake Engineering*, 42, pp. 132–136 (2012).
- [15] Kong, E., Song, J.S., Kang, B.B. and Na, S. "Dynamic response and robust control of coupled maglev vehicle and guideway system", *Journal of Sound and Vibration*, 330(25), pp. 6237–6253 (2011).
- [16] Samali, B. and Al-Dawod, M. "Performance of a five-story benchmark model using an active tuned mass damper and a fuzzy controller", *Engineering Structures*, 25, pp. 1597–1610 (2003).
- [17] Ha, Q.P. "Active structural control using dynamic output feedback sliding mode", *Proc. 2001 Australian Conference on Robotics and Automation*, Sydney, pp. 20–25 (2001).
- [18] Symans, M.D. and Kelly, W. "Fuzzy logic control of bridge structures using intelligent semi-active seismic isolation systems", *Earthquake Engineering and Structural Dynamics*, 28, pp. 37–60 (1999).
- [19] Lin, C.C., Chang, C.C. and Wang, J.F. "Active control of irregular buildings considering soil–structure interaction effects", *Soil Dynamics and Earthquake Engineering*, 30(3), pp. 98–109 (2010).
- [20] Alexandros, A.T. "Optimal probabilistic design of seismic dampers for the protection of isolated bridges against near-fault seismic excitations", *Engineering Structures*, 33(12), pp. 3496–3508 (2011).
- [21] Aldemir, U. "Predictive suboptimal semiactive control of earthquake response", *Structural Control and Health Monitoring*, 17(6), pp. 654–674 (2010).
- [22] Alhan, C., Gavin, H.P. and Aldemir, U. "Optimal control: basis for performance comparison of passive and semiactive isolation systems", *Journal of Engineering Mechanics*, ASCE, 132(7), pp. 705–713 (2006).
- [23] Pourzeynali, S., Lavasani, H.H. and Modarayi, A.H. "Active control of high rise building structures using fuzzy logic and genetic algorithms", *Engineering Structures*, 29, pp. 346–357 (2007).
- [24] Clough, R.W. and Penzien, J., *Dynamics of Structure*, second ed., Mc Graw-Hill, Inc. (1993).
- [25] Chopra, A.K., *Dynamics of Structures: Theory and Application to Earthquake Engineering*, Prentice-Hall (1995).
- [26] Pourzeynali, S. and Esteki, S. "Optimization of the TMD parameters to suppress the vertical vibrations of suspension bridges subjected to earthquake excitations", *Iranian International Journal of Engineering, IJE Transaction B (Application)*, 22(1), pp. 23–34 (2009).
- [27] Zuo, L. and Nayfeh, S. "The multi-degree-of-freedom tuned-mass damper for suppression of single-mode vibration under random and harmonic excitation" *ASME, Proceedings on Mechanical Vibration & Noise*, 5, pp. 2051–2061 (2003).
- [28] Ogata, K., *Modern Control Engineering*, Prentice-Hall of India, New Delhi (1997).
- [29] Holland, J.H., *Adaptation in Natural and Artificial Systems*, MIT Press, Cambridge, MA (1975).
- [30] Pourzeynali, S. and Mousanejad, T. "Optimization of semi-active control of seismically excited buildings using genetic algorithms", *Scientia Iranica, Transaction A: Civil Engineering*, 17(1), pp. 26–38 (2010).
- [31] Deb, K. "Single and multi-objective optimization using evolutionary computation", Department of Mechanical Engineering, Indian Institute of Technology Kanpur, KanGAL Report Number 2004002 (2004).
- [32] Srinivas, N. and Deb, K. "Multi-objective optimization using non-dominated sorting in genetic algorithm", *Evolutionary Computation*, 2(3), pp. 221–248 (1994).
- [33] Deb, K., Agrawal, S., Pratap, A. and Meyarivan, T. "A fast and elitist multi-objective genetic algorithm: NSGA-II", *IEEE Transactions on Evolutionary Computation*, 6(2), pp. 182–197 (2002).
- [34] Zitzler, E., Deb, K. and Thiele, L. "Comparison of multi-objective evolutionary algorithms: empirical results", *Evolutionary Computation*, 8(2), pp. 173–195 (2000).
- [35] Rudolph, G., "Evolutionary search under partially ordered sets", Department of science/LS11, University of Dortmund, Dortmund, Germany, Tech. Rep. CI-67/99 (1999).
- [36] Pourzeynali, S. and Zarif, M. "Multi-objective optimization of seismically isolated high-rise building structures using genetic algorithms", *Journal of Sound and Vibration*, 311, pp. 1141–1160 (2008).
- [37] Ray, L.R. and Stengel, R.F. "A Monte Carlo approach to the analysis of control system robustness", *Automatica*, 29, pp. 229–236 (1993).
- [38] Wang, Q. and Stengel, R.F. "Robust control of nonlinear systems with parametric uncertainty", *Automatica*, 38, pp. 1591–1599 (2002).
- [39] Crespo, L.G. and Kenny, S.P., "Robust control design for systems with probabilistic uncertainty", *NASA Report*, TP-2005–213531 (March, 2005).
- [40] Smith, B.A., Kenny, S.P. and Crespo, L.G., "Probabilistic parameter uncertainty analysis of single input single output control systems", *NASA Report*, TM-2005–213280 (March, 2005).
- [41] Montgomery, D.C., *Applied Statistics and Probability for Engineers*, third ed., John Wiley & Sons, Inc. (2003).
- [42] Hajiloo, A., Nariman-zadeh, N., Jamali, A., Bagheri, A. and Alasti, A. "Pareto optimum design of robust PI controllers for systems with parametric uncertainty", *International Review of Mechanical Engineering (I.R.M.E.)*, 1(6), pp. 628–640 (2007).
- [43] International Building Code, IBC (2006).
- [44] Pourzeynali, S. and Datta, T.K. "Effect of tuning frequency on TMD control of suspension bridge flutter", *Book of Abstract of the 12th Annual International Mechanical Engineering Conference, ISME2004*, 18–20 May 2004, Tehran, Iran, Tarbiat Modarres University, p. 59 (2004).
- [45] Blasco, X., Herrero, J.M., Sanchis, J. and Martinez, M. "A new graphical visualization of n -dimensional Pareto front for decision-making in multi-objective optimization", *Information Sciences*, 178, pp. 3908–3924 (2008).

Saeid Pourzeynali obtained his M.S. and Ph.D. degrees in Structural Engineering in 1989 and 2001 from Tehran University, Iran, and IIT Delhi, India, respectively. He is currently Associate Professor in the Department of Civil Engineering at the University of Guilan, Rasht, Iran. Dr. Pourzeynali has more than 20 years of teaching experience, and has published more than 80 international journal and conference papers. His research interests include: structural dynamics, earthquake engineering, random vibrations, reliability analysis, structural control and optimization, and dynamics of cable supported bridges. Dr. Pourzeynali has received various awards among which the notable one is the "2004 best research study on cable supported bridges" from the Vice-Chancellor for Research of the University of Guilan.

Shide Salimi received her B.S. degree in Civil Engineering from IKIU, Qazvin, Iran, in 2007 and a M.S. degree in Structural Engineering from the University of MAU, Ardabil, Iran, in 2011. Her main research interests include: structure design, control design, optimization, fuzzy control, and isolator design.

Houshyar Eimani-Kalehsar received his M.S. degree in Structural Engineering from the University of Tabriz, Iran, in 1990, and a Ph.D. degree in Experimental Aerodynamics on Tall Rectangular Buildings from IIT Roorkee, India, in 2000. He is currently Assistant Professor of Civil Engineering at the University of Mohaghegh-e-Ardabili, in Ardabil, Iran. He joined as a lecturer in the Dept. of Civil Engineering in May, 1990. He is a life member of Indian society for wind engineering (ISWE). He has derived non-dimensional force spectrum for estimation of crosswind response of tall rectangular buildings which is unique and useful in the above mentioned area. Dr. Eimani-Kalehsar has more than 22 years of teaching experience, and has published more than 30 international journal and conference papers. His research interests include: theory of plates and shells, bridge engineering, wind engineering, structural aerodynamics and random vibrations.